Proceedings of DOE 2003 Diesel Engine Emissions Reduction Conference
August 24-28, 2003, Newport, RI

FUEL FORMULATION EFFECTS ON DIESEL FUEL INJECTION, COMBUSTION, EMISSIONS AND EMISSION CONTROL

André Boehman, Mahabubul Alam, Juhun Song, Ragini Acharya, Jim Szybist and Vince Zello
The Energy Institute
The Pennsylvania State University
405 Academic Activities Building
University Park, PA 16802

Kirk Miller
ConocoPhillips
600 N. Dairy Ashford
Houston, TX 77252

ABSTRACT

This paper describes work under a U.S. DOE sponsored Ultra Clean Fuels project entitled "Ultra Clean Fuels from Natural Gas," Cooperative Agreement No. DE-FC26-01NT41098. In this study we have examined the incremental benefits of moving from low sulfur diesel fuel and ultra low sulfur diesel fuel to an ultra clean fuel, Fischer-Tropsch diesel fuel produced from natural gas. Blending with biodiesel, B100, was also considered. The impact of fuel formulation on fuel injection timing, bulk modulus of compressibility, in-cylinder combustion processes, gaseous and particulate emissions, DPF regeneration temperature and urea-SCR NOx control has been examined. The primary test engine is a 5.9L Cummins ISB, which has been instrumented for in-cylinder combustion analysis and in-cylinder visualization with an engine videoscope. A single-cylinder engine has also been used to examine in detail the impacts of fuel formulation on injection timing in a pump-line-nozzle fueling system, to assist in the interpretation of results from the ISB engine.

INTRODUCTION

Diesel particulate emissions pose a significant potential health hazard. Control of diesel particulate emissions is an issue requiring the attention of the fuels, engine and aftertreatment industries. To achieve the reductions in particulate emissions mandated by the US Environmental Protection Agency in 2007, use of diesel particulate filters (DPF) will be a necessity [1]. To enable the implementation of particulate and NOx control technologies, the US EPA has mandated that ultra low sulfur fuels be available to enable advanced aftertreatment strategies, which can be highly sulfur sensitive [2]. A critical requirement for implementation of diesel particulate filters on diesel-powered vehicles is having a low "break even temperature," defined as the temperature at which particulate deposition on the filter is balanced by particulate oxidation on the filter. This balance point needs to occur at sufficiently low temperatures to fit within the exhaust temperature range of a typical diesel vehicle's duty cycle. Catalytic coating on the diesel particulate filter, use of a fuel borne catalyst and oxidation catalysts placed upstream of the particulate filter can all reduce this balance point temperature. Another important factor in lowering the balance point temperature is fuel sulfur content, because the sulfur dioxide generated during combustion can poison catalyst activity [1,2].

Modification of diesel fuel composition, for example, by blending with oxygenated fuels, also can contribute to reducing emissions. Addition of biomass-derived fuels and synthetic fuels to diesel fuel basestocks is a means of producing a cleaner burning diesel fuel. Blending with oxygenated or zero sulfur fuels can lead to particulate emissions reductions by interfering with the soot formation process and by decreasing the formation of sulfates. However, in the case of biodiesel fueling (e.g., "B20", a blend of 20vol.% methyl soyate in diesel fuel) there is a well documented increase of 2-4% in NOx emissions [3]. As shown by Van Gerpen and co-workers [4,5] and Szybist and Boehman [6], the NOx increase with biodiesel fueling is attributable to an inadvertent advance of fuel injection timing. The advance in injection timing is due to the higher bulk modulus of compressibility, or speed of sound, in the fuel blend, which leads to a more rapid transferal of the pressure wave from the fuel pump to the injector needle and an earlier needle lift.

In this paper, we present results from several related studies on the impact of fuel formulation. We examine the interaction between the bulk modulus of compressibility and effect on fuel injection timing of various fuel samples. The

fuels considered include methyl soyate (the methyl ester of soybean oil), unrefined soybean oil, paraffinic solvents, and ultra low sulfur and conventional diesel fuels. Both the impact on injection timing and the variation in the bulk modulus of compressibility are measured so that correlation between fuel composition, fuel properties and injection timing can be observed and quantified.

In addition, we present comparative study of the impact of sulfur content and biodiesel blending on particulate trap operation. The means of comparison is analysis of the impact of fuel composition on the break even temperature. Work is ongoing to compare fuel effects on urea-selective catalytic reduction of NOx, but we do not report those results here.

Also, we present results from in-cylinder imaging in a Cummins 5.9L, turbocharged, six-cylinder, 4-stroke direct injection (DI) diesel engine using an engine videoscope system. The imaging studies provide a comparison of the fuel injection timing, ignition timing, spray formation and flame luminosity between different fuels. Blends of biodiesel in an ultra low sulfur diesel fuel are presented here.

Finally, we present recent experimental results on combustion and emissions of ConocoPhillips Fischer-Tropsch diesel fuel (COP F-T diesel), in comparison with conventional and biodiesel fuels. Together, these results present a mosaic of data that shed light on the potential impact of fuel formulation on injection, combustion, emissions formation and emissions control for diesel engines.

EXPERIMENTAL

Several different experimental systems were used in the work described here: a high pressure viscometer, capable of measuring the bulk modulus of compressibility with the use of a pycnometer; a highly instrumented, single-cylinder direct injection (DI) diesel engine, with an accompanying spray visualization chamber, and a highly instrumented 6-cylinder DI turbodiesel engine equipped with a catalyzed diesel particulate filter. The bulk modulus of various fuels was measured, and corresponding measurements were made of the impact of the fuel on the injection timing in the DI diesel engines.

High Pressure Viscometer. This instrument was developed for studies of the viscosity and bulk modulus of hydraulic fluids that contained dissolved gases [7]. The principle of operation for this device is that when a fluid is exposed to higher pressures, it will have a reduction in volume. The governing equation for the calculation of bulk modulus is:

$$B = (P-Po)*Vo/(Vo-V) \qquad (1)$$

where B is the bulk modulus in MPa, P is the measured pressure in MPa, Po is atmospheric pressure, Vo is the volume of the sample at atmospheric pressure and V is the volume at the new pressure.

The measurement equipment consists of a modified 21-R-30 Stainless Jerguson gage capable of handling pressures up to 4000 psi. Two panels with viewing windows allow for viewing of the sample. Each window glass has two gaskets, one on either side, to ensure a tight seal on the chamber. For pressures in the range of 0-1000 psi, a direct connection to a helium gas cylinder provides the necessary pressure. For pressures above 2000 psi, a 4.5-liter Aminco hydrogenation bomb is filled with helium and oil is pumped into the bomb to achieve pressures up to 16000 psi. A constant temperature bath kept the pressure cell at a temperature of 100 degrees F. Bulk modulus is measured via a change in height within the pycnometer tube, as the pressure in the cell is varied. Water was used as a calibration standard.

Single-Cylinder DI Diesel Engine and Spray Chamber. A Yanmar L40 AE D air cooled 4-stroke DI diesel engine was coupled to an electric motor and motored at speed and fuel consumption conditions that simulated the G2 test modes from the ISO 8178-4.2 [8]. Only results from a load setting of 25% at 3600 RPM are presented here. The experimental system is shown schematically in Figure 1. The fuel consumption was measured by a gravimetric method using an Ohaus Explorer balance, accurate to 0.1g. The fuel injector was removed from the cylinder head and placed into a spray chamber with visual access to the fuel spray. The chamber was positioned so that the original high pressure fuel line could be used without modification of length, although it was necessary to bend the fuel line. The spray timing was monitored with a light attenuation method. A Uniphase 0.95 mW Helium-Neon laser was positioned so that the laser beam intersected the fuel spray at the injector orifice. During the spray event the laser was attenuated, changing the output voltage and enabling a clear transition at both the beginning and end of the spray.

The additional single-cylinder engine tests that include ConocoPhillips Fischer-Tropsch diesel fuel were performed in a Yanmar L70 EE air-cooled, 4-stroke, single cylinder, DI diesel engine with a maximum power output of 7 hp was operated at 75% load and 3600 RPM (operating mode 2 from the ISO 8178 G2 test). Cylinder pressure and fuel-line pressures were measured using Kistler piezoelectric pressure transducer models 6052B1 and 601B1, respectively. A Hall-effect proximity sensor, installed by Wolff Controls Corporation, was used to measure needle-lift in the injector. An AVL 364 shaft encoder installed on the engine crankshaft, along with a Keithley DAS 1800 data acquisition board enabled 0.1 CA degree resolutions of these signals. NOx emissions were measured using an Eco-Physics NOx analyzer integral in an AVL GEM 110 emissions bench.

Multi-Cylinder DI Diesel Engine and Test Procedure. Tests were performed with a Cummins ISB 5.9L turbodiesel engine (MY2000, 235 HP max output) connected to a 250 HP capacity, eddy current absorbing dynamometer. The engine has been heavily instrumented, with a 0.1 crank angle resolution crank shaft encoder, a cylinder pressure sensor, a needle lift sensor and in-cylinder visualization using an AVL 513D Engine Videoscope. The engine and dynamometer are operated through an automated control system. Connected to the engine exhaust is an Engelhard catalyzed diesel particulate filter. Exhaust samples are pulled upstream and downstream of the DPF, while exhaust temperature, filter temperature and pressure drop across the DPF are monitored.

Prior to a break even temperature (BET) test, the filter is cleaned of particulate via operation at elevated temperature. Then, the exhaust temperature is reduced while the filter is filled with particulate matter until the pressure drop across the filter reaches 20 inches of H_2O. Then, exhaust temperature is increased in steps by increasing the load on the engine. Four fuel formulations were considered, a low sulfur diesel fuel (LSD, 325 ppm sulfur), ultra low sulfur diesel fuel (ULSD, 15

ppm sulfur), a 20 vol.% blend of biodiesel ("B20") with LSD (LSD/B20) and a B20 blend with ULSD (ULSD/B20).

Particulate mass measurements are obtained with a Sierra Instruments BG-1 Micro Dilution Test Stand by sampling onto Pallflex 90 mm filters. Measurement of the soluble organic fraction (SOF) of the particulate matter is performed by weighing the sample filter before and after solvent extraction using dichloromethane (DCM). Gaseous emissions were obtained with an AVL CEB II raw diesel emissions bench.

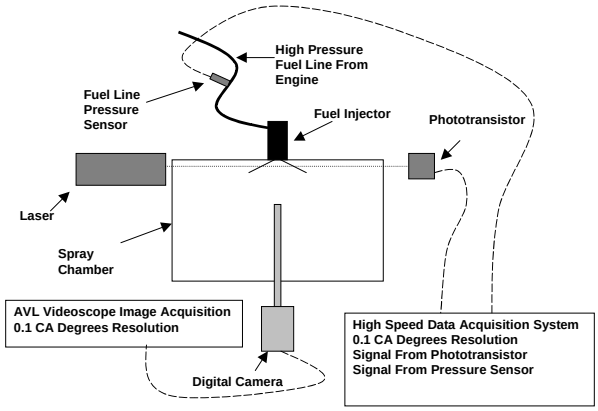

Figure 1. Schematic diagram of the spray visualization chamber connected to the DI diesel engine with access for digital imaging and laser attenuation measurements of fuel injection timing.

RESULTS AND DISCUSSION

Bulk Modulus and Injection Timing. Figures 2 and 3 show results from the measurements of injection timing and the bulk modulus of compressibility for diesel and biofuel blends. If one takes the indication of 0.4 relative spray intensity as an indication of the start of fuel injection, Figure 2 indicates that there is a 0.2 to 0.3 CA advance of fuel injection timing for the diesel-biodiesel (B20) and diesel – soy oil blends, while there is an advance of 1.0 CA with pure biodiesel (B100). Figures 3 and 4 show that the effect of purely paraffinic fuels is to retard the fuel injection timing. The injection timing is retarded for Norpar by 0.5 CA., which also has the lowest bulk modulus.

As shown in Figure 2, fuel injection timing advances of 0.3 crank angle (CA degrees) and 1 CA degree are observed in "pump-line-nozzle" configuration fuel systems, for B20 and B100 respectively. This injection timing advance in a purely mechanical fuel injection system may not be as likely in an electronically controlled fuel injection system. In the Cummins ISB engine, the Bosch fuel system is electronically controlled which complicates the interpretation of fuel effects on injection timing. As seen in Figure 5, for the LSD/B20 blend there is a 0.2 crank angle degree advance of injection timing in the Cummins ISB engine relative to the LSD. For the ULSD/B20 blend there is a 0.3 crank angle degree retardation of injection timing relative to the ULSD. The engine controller itself may shift injection timing due to differences in throttle position required to meet the required load because of differences in the calorific value and cetane number of the test fuels.

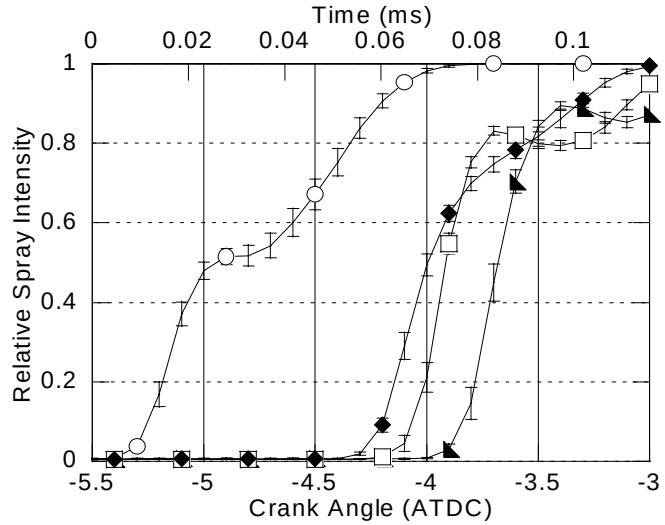

Figure 2. Measured fuel injection timing for biodiesel blends in conventional diesel fuel shown as relative spray intensity as a function of crank angle position relative to TDC. (◣) Baseline diesel fuel, (□) B20, (○) B100, (◆) 16vol.% Soy oil in diesel fuel.

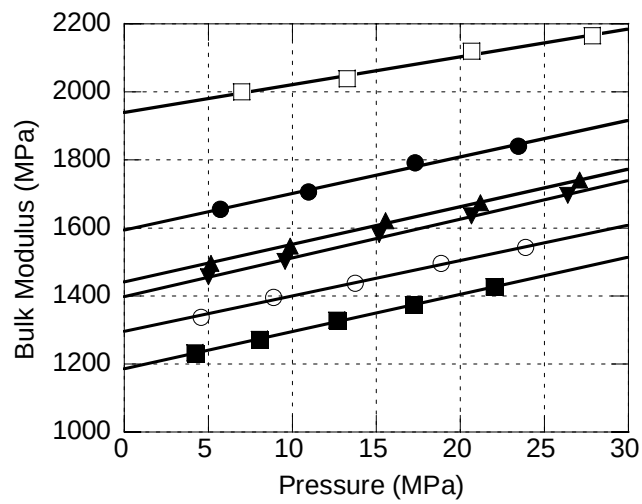

Figure 3. Measured bulk modulus of (□) Soy oil, (●) Biodiesel, B100, (▲) 20% biodiesel blend in BP15 diesel fuel, B20, (▼) BP15 diesel fuel and (○) ConocoPhillips Fischer-Tropsch diesel and (■) Norpar-13 as a function of pressure.

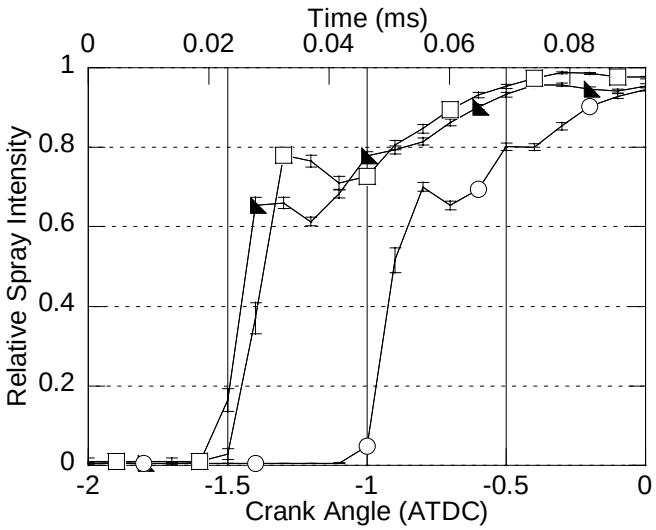

Figure 4. Measured fuel injection timing for paraffinic fuels versus conventional diesel fuel shown as relative spray intensity as a function of crank angle position relative to TDC. (◣) 15 ppm sulfur diesel fuel (BP15), (□) 325 ppm sulfur diesel fuel, and (○) Norpar-13.

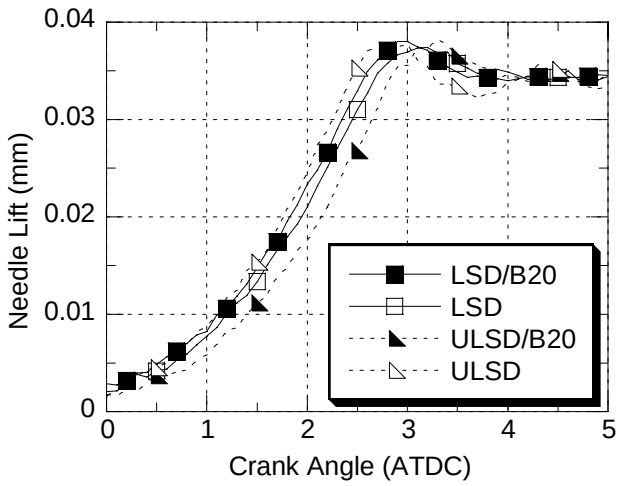

Figure 5. Influence of fuel composition on injection timing in the Cummins ISB engine during the particulate filter loading process.

Diesel Particulate Filter Regeneration. Figure 6 shows the particulate composition during the filter loading period and indicates that there are some modest differences in the rate and composition of the particulate that is depositing on the DPF.

Figure 7 shows the variation of engine-out NOx emissions during the filter regeneration process, caused by the differences in fuel composition and the presence of biodiesel fuel. Figure 8 shows the extent of conversion of engine-out NO to NO_2 across the catalyzed DPF due to oxidation although some NO reacts with other exhaust species such as hydrocarbons leading to a slight loss in downstream NO. Figure 9 indicates the variation in break even temperature with test fuel composition. The BET is determined by following the slope in the variation of pressure drop as exhaust temperature increases.

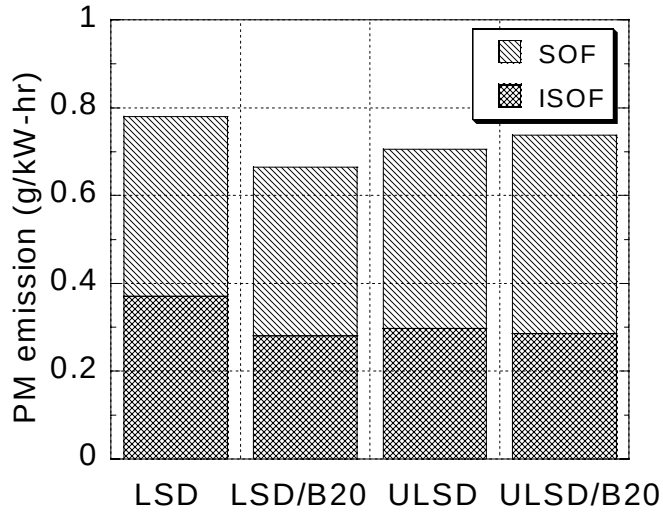

Figure 6. Particulate composition during the filter loading process for the various test fuels.

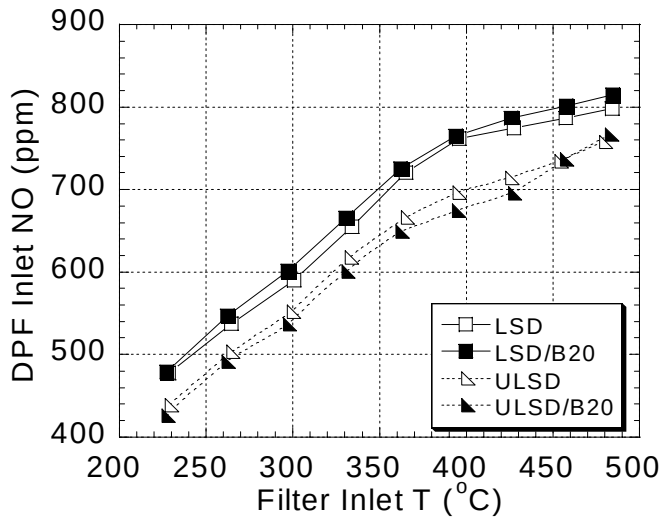

Figure 7. Variation in engine-out NOx emissions during the filter regeneration process for the various test fuels.

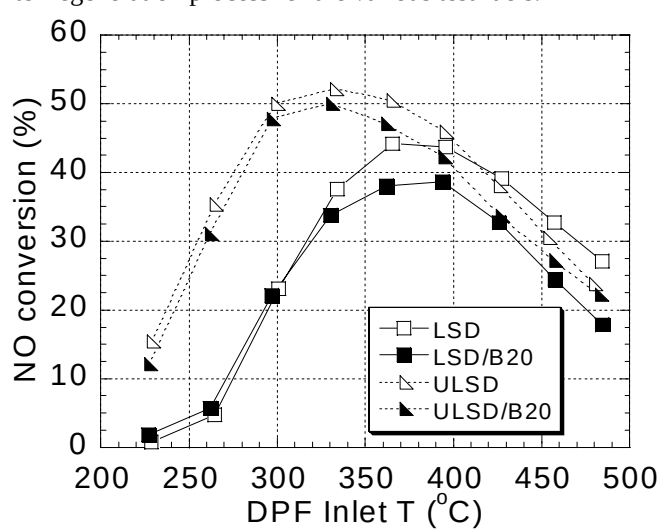

Figure 8. Variation in NO conversion to NO_2 across the DPF during the filter regeneration process for the various test fuels.

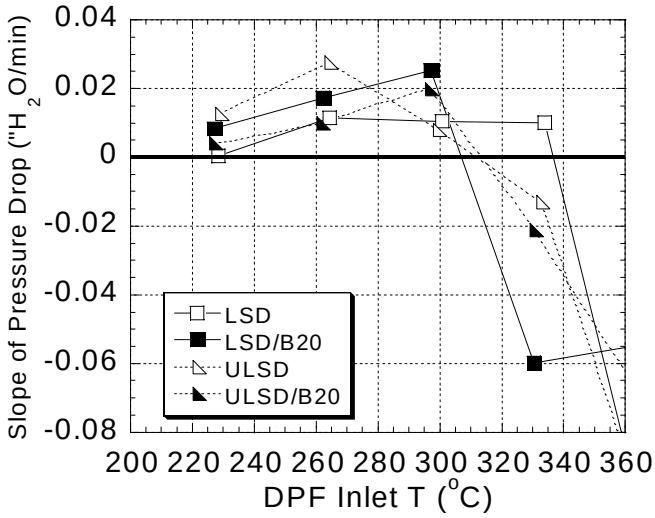

Figure 9. Filter temperature versus slope of the pressure drop, indicating the break even temperature for the various test fuels.

The results in Figures 6-9 show that although there is modest variation in the composition and mass emissions rate of particulate matter from the engine between the test fuels, there are differences in engine-out NOx and, as a consequence, NO conversion across the catalyzed DPF. For both base fuels, the LSD and ULSD, there is an engine-out increase in NOx, which is comprised mostly of NO. Subsequently, the engine-out NO is oxidized to NO_2 over the catalyst that is impregnated into the DPF. The NO_2 assists in the oxidation of the particulate matter on the DPF, because NO_2 is a more aggressive oxidizer of diesel particulate matter than O_2 [1]. However, the conversion of NO to NO_2 is inhibited by the presence of SO_2 in the exhaust, which is 20 times higher for the LSD than for the ULSD. So, the NO conversion to NO_2 is lower and requires an additional 35°C exhaust temperature to become significant for the LSD due to its higher sulfur content.

Of great interest is that the net effect of the higher engine-out NOx emissions and 20% reduction in fuel sulfur content for the LSD/B20 fuel leads to the lowest break even temperature, 308°C. Consistent with one's expectations, the LSD has the highest BET. However, the ULSD and ULSD/B20 fuels yield the same BET. This difference in BET may be explained by the generally lower NOx emissions for the ULSD and ULSD/B20 fuels relative to the LSD and LSD/B20 fuels. There is more NOx with the LSD and LSD/B20 fuels to serve to oxidize the particulate matter on the DPF after conversion of NO to NO_2, but for the LSD the NO conversion is inhibited and the particulate oxidation is inhibited by the higher sulfur content.

In-Cylinder Imaging of Biodiesel Combustion. Engine cylinder number six was selected for optical access and the cylinder head modified accordingly. An AVL 513D Videoscope was used for capturing images of spray and combustion [9]. Optical access to the combustion chamber was obtained by installing two small windows in the cylinder head. The windows permit access for an external light source through one window and an endoscope through the other. The videoscope system is an integrated triggering and digital imaging system. The triggering system was operated with an AVL 364 angle encoder mounted on the engine crankshaft, enabling 0.1 crank angle (CA) degree resolution. A xenon bulb was used to illuminate the cylinder with a flash duration of 30 µs, and a radiometric light output of 328 mJ per flash. The image exposure duration was 62 µs. This videoscope system was only able to take one image per power cycle. Therefore, the images rely on cycle to cycle repeatability. The AVL videoscope system includes post-processing software for image processing and analysis, which was used to obtain the data presented here.

Three types of fuels were considered to perform these experiments. An ultra low (BP-15) sulfur diesel fuel with 15 ppm sulfur was considered as base fuel for blending with biodiesel. Neat biodiesel (B-100) and a blend of 20 wt.% biodiesel (B-20) with the base fuel were used. Tests were performed at steady state condition and the test engine was operated with 10% rated load (40 ft-lbs torque) at a constant speed of 1800 rpm. The control system was programmed so as to reach the desired speed and load in less than 10 seconds. Once the engine reached the desired speed and load, the spray and combustion images were taken and saved into the AVL high speed data acquisition system. Simultaneously, cylinder pressure and needle lift data were recorded for combustion and heat release analysis.

The following is a qualitative and quantitative analysis of the spray and combustion characteristics of ultra low sulfur diesel fuel (BP-15), neat biodiesel (B-100) and the biodiesel (B-20) blend. Figure 10 presents different combustion events for all the fuels starting from TDC to 30 deg ATDC at an interval of 3.0 CAD. Figure 10 mainly shows the evolution of the spray and combustion for one of the seven spray jets of the fuel injector for each of the three fuels. The bright spot on the right of the images behind the injector tip is the light source that was used to illuminate the spray. The images of the spray and combustion were at a light load condition. Therefore,

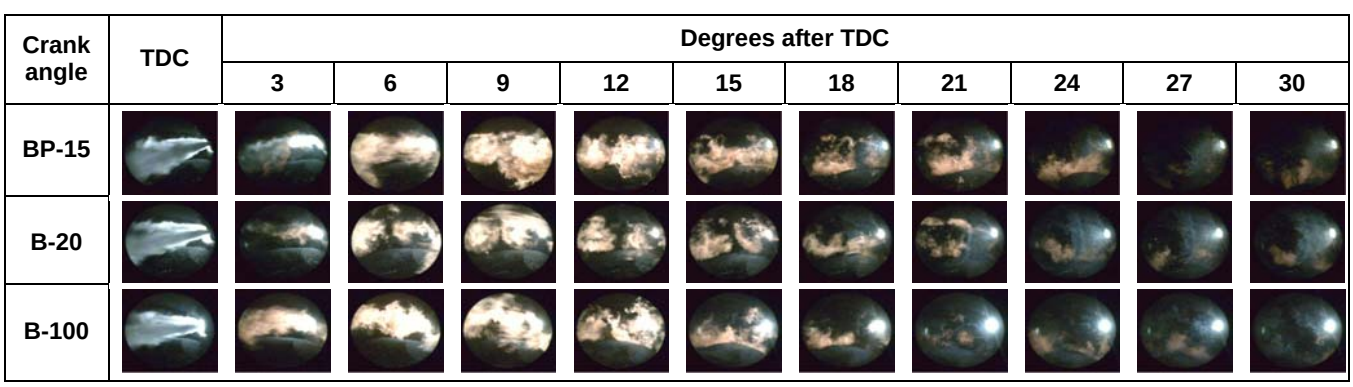

Figure 10. Combustion images from TDC to 30 deg ATDC of the combustion process with 3.0 CAD intervals

combustion was mainly controlled by the premixed burning phase. Although both the B-20 and B-100 contain fuel oxygen, it is difficult to distinguish between the spray flames of B-20, B-100 and the base diesel fuel. Also, the flames with oxygen present in the fuel were still luminous, unlike the observations by Beatrice et al. of non-luminous flames with oxygenates [10]. However, the fuel oxygen content with B-20 is 2.2 wt.% O2 and with O-20 is 11 wt.% O_2. This is much lower than the 38 wt.% threshold for "smokeless" combustion identified by Miyamoto et al. [11, 12].

Injection Timing, Combustion and Emissions with ConocoPhillips Fischer-Tropsch Fuel. Some analyses were performed with the Fischer-Tropsch diesel fuel produced at the ConocoPhillips demonstration-scale GTL plant in Ponca City, OK. Some relevant fuel property measurements are presented in Table 1. Others are shown in Figure 3, which includes the bulk modulus measurement for the COP F-T diesel. Two important pieces of information are the cetane number of the F-T diesel, CN = 83, and that the bulk modulus of the F-T diesel is below that of the base diesel fuel, which leads to retarded injection timing.

Fuel	Cetane Number	Viscosity @40 C, cSt	Flash Point, °F
BP-15 ULSD	49.7	2.5	147
BP-325 LSD	46.8	2.5	146
BP-15 /B20	52.5	2.7	151
BP-325 /B20	49.2	2.7	154
COP F-T Diesel	83	2.5	166

Table 1. Fuel Properties for Injection Timing Study

In these analyses, the Yanmar L70EE DI diesel engine was used to examine the impact on injection timing from the variation in bulk modulus of compressibility between the test fuels and the impact of cetane number of the ignition of the fuels given the variation of injection timing. The engine was operated at two conditions, 25% of full load and 75% of full load at a speed of 3600 rpm. The engine was also operated at three different fuel injection timing settings, by insertion of shims between the injection pump and engine block, referred to as "early," "mid," and "late" injection. The results, presented in Figures 11-21, include needle lift signal, heat release, NOx and CO emissions, and brake specific fuel consumption (BSFC).

In Figure 11, the linear relationship between fuel injection timing and NOx emissions is displayed for the test fuels. One can also see that the "B20" blends of either the BP15 ultra low sulfur diesel fuel or the COP F-T diesel fuel shift to earlier injection timing and higher NOx emissions.

In Figures 12-14, needle lift and heat release measurements are shown for the three injection timing settings and the four test fuels. For the "early" injection timing shown in Figure 12, the injection of both of the B20 blends is advanced and the injection of both of the F-T fuels is retarded relative to the BP15 fuels. As seen in the heat release profiles, the start of combustion is advanced for the F-T fuels relative to the BP15 fuels, due to the high cetane number of the COP F-T diesel, despite the retarded injection timing for the F-T fuels. The heat release shows a significantly higher peak pressure for the BP15 fuels due to the longer ignition delay. For the "late" injection timing in Figure 13, the peak pressures for the BP15 fuels are

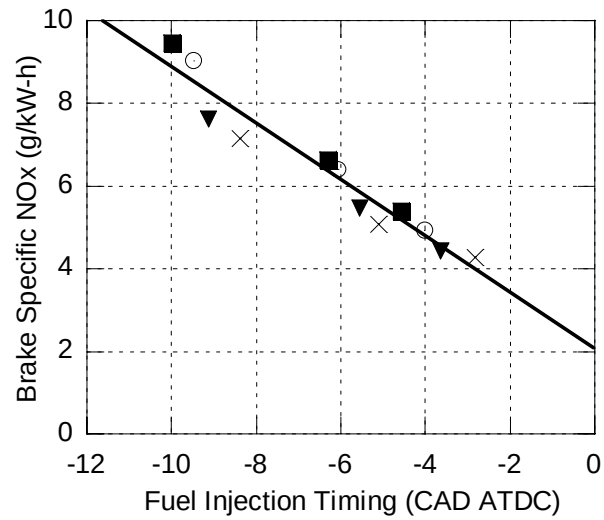

Figure 11. NOx emissions versus fuel injection timing for the various test fuels, based on three settings of static injection timing, in a Yanmar L70 DI diesel engine. (○) BP15 ultra low sulfur diesel fuel, (■) B20 blend in BP15, (×) COP Fischer-Tropsch diesel fuel, and (▼) B20 blend in COP F-T diesel.

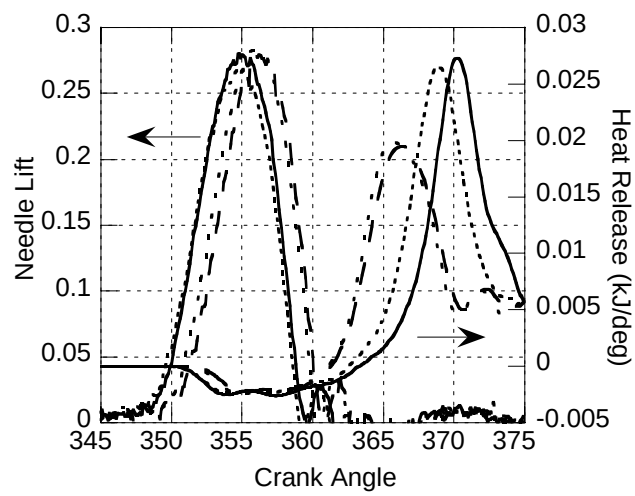

Figure 12. Needle lift and heat release versus crank angle for the "early" static injection timing at 25% load and 3600 rpm, in a Yanmar L70 DI diesel engine. (—) BP15 ultra low sulfur diesel fuel, (---) B20 blend in BP15, (— —) COP Fischer-Tropsch diesel fuel, and (- - -) B20 blend in COP F-T diesel.

lower and the start of combustion is delayed. The heat release profile shows evidence of degraded combustion for the conventional diesel fuels. However, despite the "late" injection timing and the additional retardation of injection of the F-T fuels, the heat release peak for the F-T fuels is still sharp.

The NOx and CO emissions clearly show that the effects of these variations in injection timing and cetane number. In Figure 14, at the "early" injection timing setting the NOx levels for BP15 and the COP F-T diesel are the same and slightly higher for both B20 blends. At the "mid" and "late" injection

timing settings, the COP F-T diesel and F-T/B20 blend show higher NOx that the BP15 and BP15/B20 blend. However, as seen in Figures 15 and 16, the CO emissions and BSFC are higher for BP15 and BP15/B20 than the COP F-T diesel and F-T/B20. So, the COP F-T diesel permits retarded injection timing without a penalty on CO emissions and fuel consumption, on a mass basis. Since the density of the COP F-T diesel is lower than for conventional and ultra low sulfur diesel fuels, the volumetric fuel consumption will be higher for the COP F-T fuel.

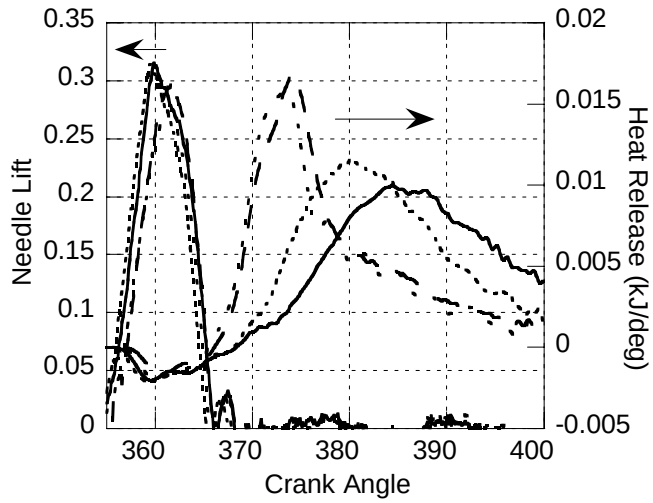

Figure 13. Needle lift and heat release versus crank angle for the "late" static injection timing at 25% load and 3600 rpm, in a Yanmar L70 DI diesel engine. (—) BP15 ultra low sulfur diesel fuel, (---) B20 blend in BP15, (— —) COP Fischer-Tropsch diesel fuel, and (- - -) B20 blend in COP F-T diesel.

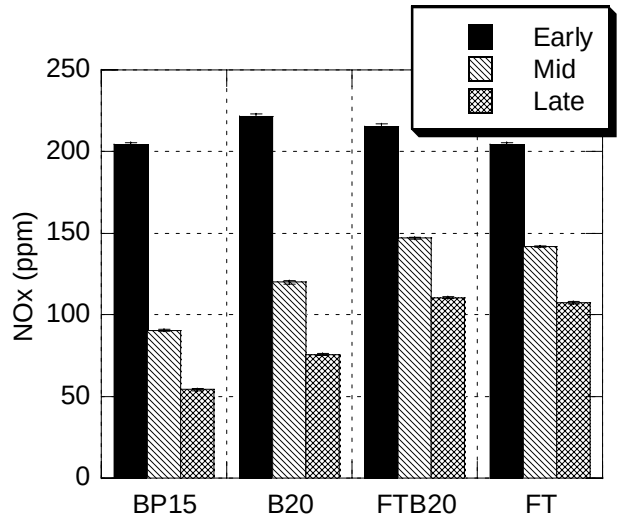

Figure 14. NOx emissions for three injection timing settings at 25% load and 3600 rpm for BP15 ultra low sulfur diesel fuel, a B20 blend in BP15, COP Fischer-Tropsch diesel fuel, and B20 blend in COP F-T diesel.

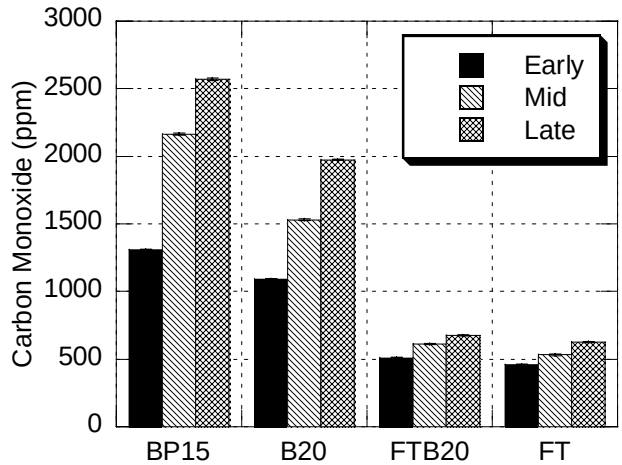

Figure 15. CO emissions for three injection timing settings at 25% load and 3600 rpm for BP15 ultra low sulfur diesel fuel, a B20 blend in BP15, COP Fischer-Tropsch diesel fuel, and B20 blend in COP F-T diesel.

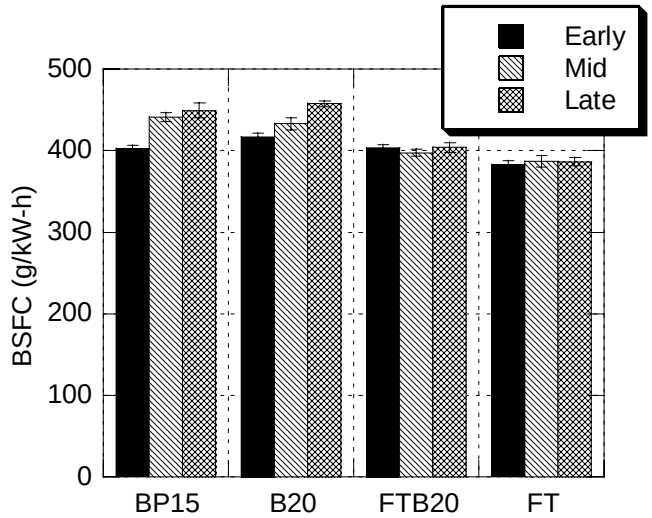

Figure 16. Brake specific fuel consumption for three injection timing settings at 25% load and 3600 rpm for BP15 ultra low sulfur diesel fuel, a B20 blend in BP15, COP Fischer-Tropsch diesel fuel, and B20 blend in COP F-T diesel.

Similar trends are observed in Figures 17 and 18 at 75% load as were observed in Figures 12 and 13 at 25% load. For the ultra low sulfur diesel fuel, BP15, combustion is delayed as injection is delayed leading to degraded combustion. The higher cetane number of the COP F-T diesel causes the F-T diesel and F-T/B20 blend to perform well despite retarded injection timing. As Figures 19, 20 and 21 show, emissions and fuel consumption are adversely affected by retarding injection timing for BP15 and BP15/B20, while the COP F-T diesel and F-T/B20 blend maintain lower emissions and lower fuel consumption.

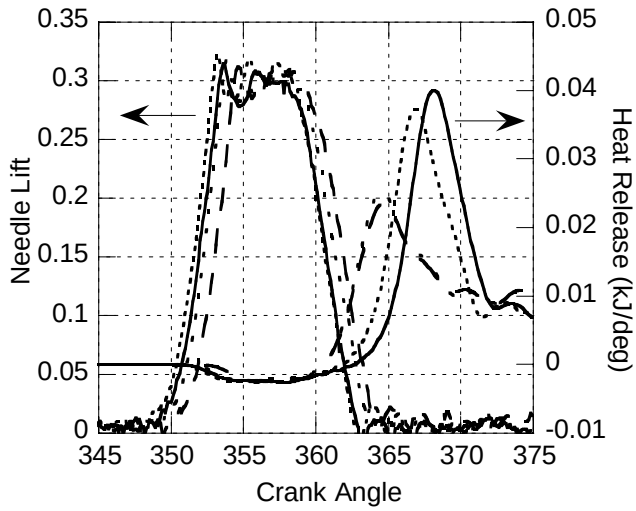

Figure 17. Needle lift and heat release versus crank angle for the "early" static injection timing at 75% load and 3600 rpm, in a Yanmar L70 DI diesel engine. (—) BP15 ultra low sulfur diesel fuel, (---) B20 blend in BP15, (— —) COP Fischer-Tropsch diesel fuel, and (- - -) B20 blend in COP F-T diesel.

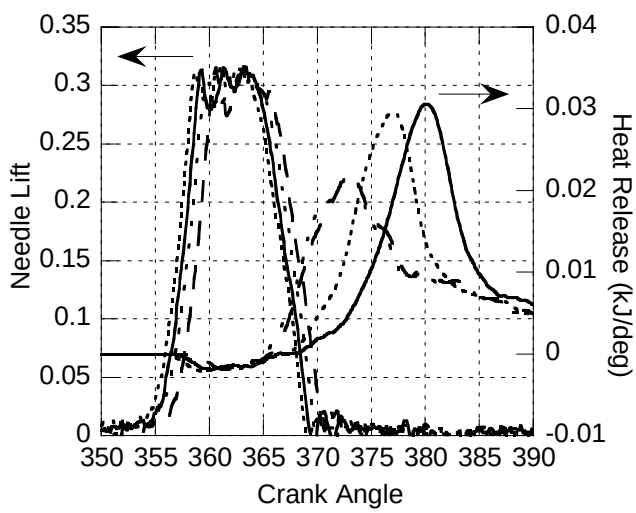

Figure 18. Needle lift and heat release versus crank angle for the "late" static injection timing at 75% load and 3600 rpm, in a Yanmar L70 DI diesel engine. (—) BP15 ultra low sulfur diesel fuel, (---) B20 blend in BP15, (— —) COP Fischer-Tropsch diesel fuel, and (- - -) B20 blend in COP F-T diesel.

CONCLUSIONS

The present work confirms previous observations on the impact of biodiesel fuels on fuel injection timing, that the higher bulk modulus of compressibility of vegetable oils and their methyl esters leads to advanced injection timing. This has been shown in the literature to contribute to the well-documented NOx emissions increase with the use of biodiesel fuel. An opposite trend is observed with paraffinic fuels, which lead to a retarding of injection timing because they have a lower bulk modulus of compressibility than conventional diesel fuels and which supports the observation that paraffinic fuels such as Fischer-Tropsch diesel fuels yield lower NOx emissions.

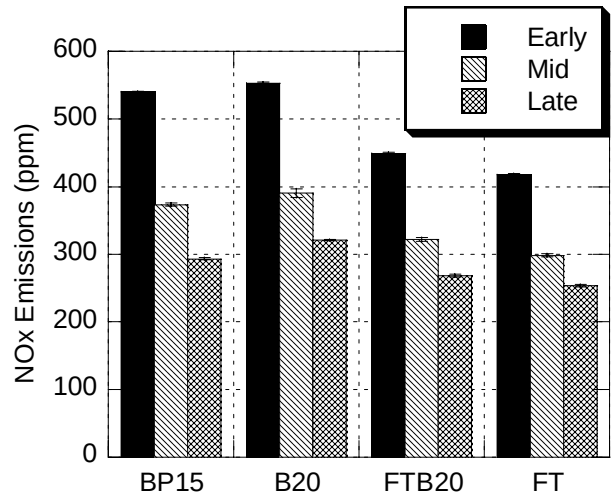

Figure 19. NOx emissions for three injection timing settings at 75% load and 3600 rpm for BP15 ultra low sulfur diesel fuel, a B20 blend in BP15, COP Fischer-Tropsch diesel fuel, and B20 blend in COP F-T diesel.

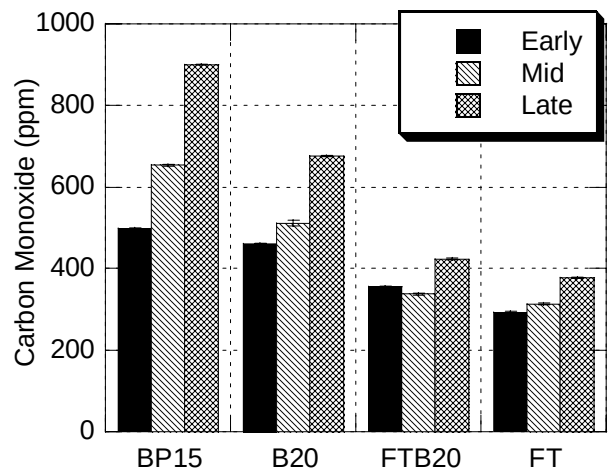

Figure 20. CO emissions for three injection timing settings at 75% load and 3600 rpm for BP15 ultra low sulfur diesel fuel, a B20 blend in BP15, COP Fischer-Tropsch diesel fuel, and B20 blend in COP F-T diesel.

While there is ample evidence in the literature of the deleterious effects of sulfur on aftertreatment devices, the results presented here show that other fuel related phenomena can have just as significant an effect on the performance of an aftertreatment device. In this specific case, the lowest break even temperature for a catalyzed DPF was observed with biodiesel blended into a low sulfur fuel.

In-cylinder visualization of the combustion of diesel and biodiesel fuels showed little change in flame luminosity and spray and flame structure as compared with ultra low sulfur diesel fuel. However, the in-cylinder imaging did provide information on shifts in injection timing, start of combustion and ignition delay that confirm needle lift and cylinder pressure trace results.

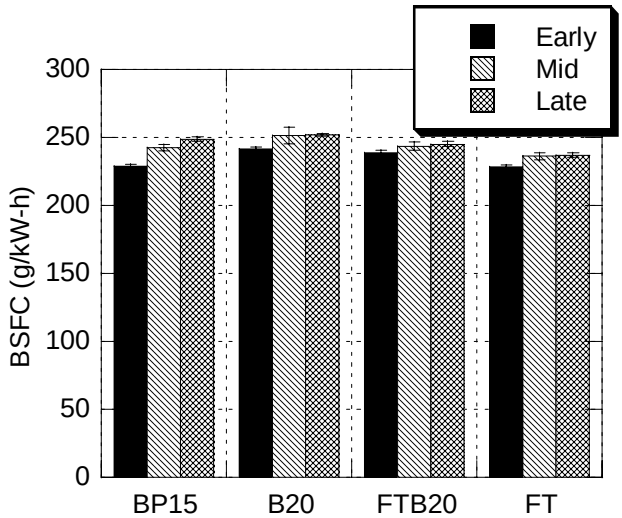

Figure 21. Brake specific fuel consumption for three injection timing settings at 75% load and 3600 rpm for BP15 ultra low sulfur diesel fuel, a B20 blend in BP15, COP Fischer-Tropsch diesel fuel, and B20 blend in COP F-T diesel.

Finally, the ConocoPhillips Fischer-Tropsch diesel fuel possesses a very high cetane number and this permits combustion with highly retarded timing, giving the opportunity to operate the engine with lower in-cylinder NOx formation.

ACKNOWLEDGMENTS

The authors with to thank the National Energy Technology Laboratory and project manager Dan Cicero for their support of this work. The authors wish to thank ConocoPhillips for its support of this work and Rafael Espinoza, Keith Lawson, Ed Casey and Etop Esen of ConocoPhillips for their technical guidance. The authors also wish to thank Vinod Duggal, Edward Lyford-Pike and John Wright of Cummins Engine Company for their support and assistance with this project. In addition, the authors thank Ken Voss and Joe Patchett of Engelhard Corporation for their support of this work.

This paper was written with support of the U.S. Department of Energy under Cooperative Agreement No. DE-FC26-01NT41098. The Government reserves for itself and others acting on its behalf a royalty-free, nonexclusive, irrevocable, worldwide license for Governmental purposes to publish, distribute, translate, duplicate, exhibit, and perform this copyrighted paper.

This material was prepared with the support of the Pennsylvania Department of Environmental Protection. Any opinions, findings, conclusions, or recommendations expressed herein are those of the author(s) and do not necessarily reflect the views of the DEP.

REFERENCES

[1] Allansson, R., P.G. Blakeman, B.J. Cooper, H. Hess, P.J. Silcock and A.P. Walker, “Optimising the Low Temperature Performance and Regeneration Efficiency of the Continuously Regenerating Diesel Particulate Filter (CR-DPF) System,” SAE Paper 2002-01-0428, 2002.

[2] Schmidt, D., V.W. Wong, W.H. Green, M.A. Weiss and J. B Heywood, “Review and Assessment of Fuel Effects and Research Needs in Clean Diesel Technology,” ASME ICE-Vol 36-1, 2001, p. 23-36.

[3] Graboski, M.S. and R.L. McCormick, “Combustion of Fat and Vegetable Oil Derived Fuels in Diesel Engines.” Progress in Energy and Combustion Science, 1998, 24(2): p. 125-164.

[4] Monyem, A., J.H. Van Gerpen, and M. Canakci, “The Effect of Timing and Oxidation on Emissions from Biodiesel-Fueled Engines”. Transactions of the ASAE, 2001, 44(1): p. 35-42.

[5] Tat, M.E., J.H. Van Gerpen, S. Soylu, M. Canakci, A. Monyem, and S. Wormley, “The Speed of Sound and Isentropic Bulk Modulus of Biodiesel at 21 degrees C from Atmospheric Pressure to 35 MPa.” Journal of the American Oil Chemists Society, 2000, 77(3): p. 285-289.

[6] Szybist, J.P. and A.L. Boehman, “Behavior of a Diesel Iinjection System with Biodiesel Fuel,” SAE Paper No. 2003-01-1039, 2003.

[7] O’Brien, J.A., “Precise Measurement of Liquid Bulk Modulus,” M.S. Thesis, Penn State University, 1963.

[8] International Organization for Standardization, ISO 8178: Reciprocating internal combustion engines - Exhaust emissions measurement - Part 4. Test Cycles for different engine applications. 1995.

[9] Werlberger, P., and Cartellieri, W. P., “Fuel Injection and Combustion Phenomena in a High Speed DI Diesel Engine Observed by Means of Endoscopic High Speed Photography”, SAE Paper 870097, 1987.

[10] Beatrice, C., Bertoli, C., and Giacomo, N. D., “New Findings on Combustion Behavior of Oxygenated Synthetic Diesel Fuels”, Combustion Sci. and Tech., Vol. 137, P 31-50, 1998.

[11] Nabi, M. N., Minami, M., Ogawa, H., and Miyamoto, N., “Ultra Low Emission and High Performance Diesel Combustion with Highly Oxygenated Fuel”, SAE Paper 2000-01-0231, 2000.

[12] Ogawa, H., Nabi, M. N., Minami, M., Miyamoto, N., and Bong-Seock, K., “Ultra Low Emissions and High Performance Diesel Combustion with a Combination of High EGR, Three-way Catalyst, and a Highly Oxygenated Fuel, Dimethoxy Methane (DMM)”, SAE Paper 2000-01-1819, 2000.